Bulletin of Faculty of Science, Zagazig University (BFSZU)
e-ISSN: 1110-1555
Volume-2024, Issue-1, pp-143-155
https://bfszu.journals.ekb.eg/journal
Research Paper DOI: **0.21608/bfszu.2023.233901.1304**

==========

A review of computational studies and bioinformatics analysis of effective drug as an inhibitor against EGFR/VEGFR-2 kinases

Mona H. Ibraheim[a], Ibrahim Maher[b], Ibrahim Khater[c]

a Physics Department, Faculty of Science, Zagazig University, P.O.44519, Zagazig, Egypt.
mhmekky@yahoo.com
b Physics Department, Faculty of Science, Zagazig University, Zagazig, Egypt. imaher@science.zu.edu.eg
c Biophysics Department, Faculty of Science, Cairo University, Giza, Egypt. ikhater@sci.cu.edu.eg
.**Corresponding author:** imaher@science.zu.edu.eg

***ABSTRACT*: Endothelial cells from cancerous tissues that express the VEGFR-2 (vascular endothelial growth factor receptor-2) start up a cascade of signaling pathways that promote tumor angiogenesis and improve cancer cell proliferation, survival, vascular permeability, and migration. Vascular endothelial growth factor (VEGF) and its receptor are important factors in physiological and pathologic angiogenesis, which has been associated with the growth and development of metastases in cancer. Through several signaling systems, EGFR (epidermal growth factor receptor) regulates cell growth, proliferation, and death. By using molecular docking drug-likeness models, pharmacokinetic, interaction analysis, and molecular dynamic simulation, the aim is to discover new inhibitors for EGFR and VEGFR-2 kinases. About 16 ligands were obtained from the drug bank and were tested against the 2 kinases by molecular docking mechanism. The compound 3C produced the highest docking score, better drug-likeness score, important pharmacokinetic properties, and strong interaction between 3C and amino acids of the 2 kinases. To evaluate the stability of the EGFR and VEGFR-2 kinases-2C complexes, molecular dynamic simulation was also performed. the stability was investigated by RMSD, Rg, and number of Hydrogen bonds. So, Inhibiting the signaling pathway of proteins that play a crucial role in the growth of cancer may be possible using compound 3C.**

***KEYWORDS:* molecular docking, EGFR, VEGFR-2, molecular dynamic simulation.**

Date of Submission: 03-09-2023 Date of acceptance: 24-09-2023

I. INTRODUCTION

According to data from the World Health Organization, cancer has been a significant global problem, as well as HIV and COVID-19 (Mohassab et al., 2021). There have been over 19 million additional cases of cancer reported, and over 10 million deaths due to cancer predicted in 2021 (Organization, 2020). To prevent cancer from spreading, nations with advanced technology must make efforts to provide cancer-related care and treatment options. The most popular of these therapies is chemotherapy because it avoids or slows the expansion of cancer cells, which typically proliferate and divide quickly (N.C.I., 2023). Inhibiting tyrosine kinases (TKs), which are important for cell division and proliferation, is one of the effective methods for treating cancer (Zhao et al., 2021). Tyrosine kinases are a category of protein kinases that play a role in the control of several physiological and biochemical processes, such as cell division, growth, and death (Drake, Lee, & Witte, 2014). Uncontrolled RTK signaling has been shown to play a key part in the formation and spread of many tumors in addition to their function in regulating normal cellular activities, which offers a basis for the production of anti-RTK drugs (Drake et al., 2014; Liang et al., 2021).

Vascular endothelial growth factors (VEGFs) are a category of tyrosine kinases that act biologically by binding in an overlapping manner with the kinase domains of three separate but structurally connected VEGF receptors (VEGFRs 1-3) (Otrock, Makarem, & Shamseddine, 2007). On the outside of blood vessels, angiogenesis-related receptor tyrosine kinases like VEGFR-2 act as crucial modulators of angiogenic features like proliferation, permeability, migration, and survival (Musumeci, Radi, Brullo, & Schenone, 2012; Sarabipour, Ballmer-Hofer, & Hristova, 2016). Drugs that directly target the growth, spread, and survival-promoting proteins found in

cancer cells, such as vascular endothelial growth factor (VEGF), human epidermal growth factor receptor type 2 (HER2), and epidermal growth factor receptor (EGFR), are used in targeted drug therapy (Larsen, Ouaret, El Ouadrani, & Petitprez, 2011). The EGFR protein controls cell migration, differentiation, and proliferation (Wieduwilt & Moasser, 2008).

A lack of control of these receptors is the cause of numerous human disorders, including cancer (Sigismund, Avanzato, & Lanzetti, 2018). There is evidence that EGFR overexpression has a major impact on the appearance and growth of several aggressive varieties of breast cancer (Schlam & Swain, 2021). VEGF is a critical regulator of physiological angiogenesis during embryogenesis, skeletal growth, and reproductive activities. Additionally, abnormal angiogenesis in tumors and other disorders has been connected to VEGF. As a result, anti-VEGF drugs are actively being examined as possible cancer treatments, either as substitutes for or additions to standard chemo or radiation therapy (Ferrara, Gerber, & LeCouter, 2003).

As a result, both EGFR and VEGFR are thought to be targets in preventing this unusual proliferation as well as in antiangiogenic techniques used in cancer therapy. Recently, drugs such as afatinib, erlotinib, gefitinib, brigatinib, and icotinib have been employed as effective anticancer medicines for lung cancer. These drugs work by blocking epidermal growth factors to provide their therapeutic benefits. First-generation quinazoline-based ATP competitive inhibitors like erlotinib, which act against the EGFR L858R and G719S mutations, have demonstrated efficacy in treating NSCLC patients (Liao, Lin, & Yang, 2015; Sullivan & Planchard, 2017).

A subfamily of the VEGFR family called VEGFR-2 suggests mediating nearly each of the cellular reactions known to occur in response to vascular epidermal growth factor (Holmes, Roberts, Thomas, & Cross, 2007). VEGF levels are noticeably greater in patients with aggressive TNBC (Linderholm et al., 2009), which suggests that TNBC tumors might be treated with anti-VEGF/VEGFR2-targeted medicines. Research has shown that blocking VEGFR-2 boosts the lethal effects of EGFR inhibitors while activating VEGFR-2 speeds up tumor growth independently of EGFR signaling and makes it easier for EGFR drug resistance to develop. Vandetanib (Caprelsa VR) is an illustration of an FDA-approved quinazoline-based drug with dual EGFR and VEGFR-2 inhibiting action (Sarkar et al., 2010).

In this work, several combined EGFR and VEGFR-2 inhibitors with effective anti-proliferative properties were chosen for pharmacophore development. The best compound's interactions with the EGFR and VEGFR-2 binding sites were demonstrated in detail using in silico techniques such as molecular docking and molecular dynamics simulation. Erlotinib is a chosen inhibitor of EGFR, sorafenib is a chosen inhibitor of VEGFR-2, and Vandetanib is a dual inhibitor of both receptors. To be aware of the chemicals' drug-like properties Before generating of the new compounds in the lab, the pharmacokinetic characteristics of the intended dual inhibitors were also predicted. The primary pharmacokinetic characteristics of ADMET (adsorption, distribution, metabolism, excretion, and toxicity) were chosen as the drug-likeness criteria in this study.

II. MATERIALS AND METHODS

2.1 Protein selection and preparation

In the process of angiogenesis, the kinases EGFR and VEGFR-2 are crucial. The determined structures for EGFR and VEGFR-2 were taken from the protein data bank (PDB ID: 8A27 and 4ASD, respectively) and were shown in the crystal structure of the EGFR and VEGFR-2 kinases, then PyMol software removed ligands, heteroatoms and water molecules (Schrodinger, 2021) to perform molecular docking analysis.

2.2 Ligands Optimization

The ligand structure was obtained via the web Drugs Bank about 16 ligands, an extensive database of chemical effects, and drug target characteristics (Wishart et al., 2017). (https://avogadro.cc) Avogadro was programmed to create each inhibitor with the best possible design, MMFF94, a force field function, was utilized (Hanwell et al., 2012) and then saved in PDB format.

2.3 Molecular Docking Analysis

The molecular docking was carried out using the Auto Dock Vina program (http://vina.scripps.edu) with the default parameters (Trott & Olson, 2010). The protein structure's amino acid residues were given polar hydrogen atom additions, followed by Kollman charges, to carry out a molecular docking analysis using the auto dock vina software (Morris et al., 2009). The VEGFR-2 binding pocket's active site are Cys919, Leu840, Phe918, Gly922, Glu917, Val 916, Lys 868, Asp1046, Phe1047, 1048, Leu889, Leu1019, Ile892, Ile888, Val899, and Ile1044, on the other hand, The EGFR active site residues are Leu 718, Gly 721, Thr 790, Met 793, Gly 796, Cys 797, ASP 800, Asp 831, Arg 841, Thr 854, Asp 855, and Phe 856 (Usui, Ban, Kawada, Hirokawa, & Nakamura, 2008). The grid box for forVEGFR-2 kinase at: CyY: -9, Leu840, Phe918, Gly922, Glu917, Val 916, Lys 868, Asp1046, Phe1047, 1048 , Leu889, Leu1019, Ile892, Ile888, Val899, and Ile1044 with coordinates X:-5.778, Y:3.500 and Z:-7.639(A0) and dimensions of X:72, Y:70 and Z:76 while for EGFR

kinase at Leu718, Gly721, Thr790, Met 793, Gly796, Cys797, ASP800, Asp831, Arg 841, Thr854, Asp 855, and Phe856 with coordinates of X:11.194, Y:-8.333, any Z:-14.083(A0) and dimensions of X:72, Y:78 and Z:76 then the docking process carried out.

2.4 Drug likeness Score and Pharmacokinetic (ADME) of drug

Using information from the web server Molsoft (http://molsoft.com/mprop/), which determines drug-likeness based on the Blood-Brain Barrier value (BBB), the total number of hydrogen bond acceptors, molecular weight and the total number of hydrogen bond donors each compound's drug-likeness was determined. The PreADMET and SwissADME websites were utilized online in predicting the ADME of bioactive substances. Based on the chemical constitution of the drug, these PreADMET and SwissADME services (http://preadmet.bmdrc.org) determine pharmacokinetic parameters including BBB (Cblood/CBrain), plasma protein binding, toxicity prediction, and human intestinal absorption percentage.

2.5 Analysis of Proteins and ligand interactions

The Protein-Ligand Interaction Profiler (PLIP) website was used to examine the interactions between the EGFR and VEGFR-2 kinases and their ligands. Protein-ligand interaction patterns are discovered and displayed using the PLIP web tool from 3D structures which showed Hydrophobic Interactions, Hydrogen Bonds, π-Cation Interactions, and Halogen Bonds.

2.6 Molecular dynamics simulation analysis

For the MD simulation, the Auto Dock docking configuration with the lowest binding energy was used as an initial conformation. The molecular dynamics simulation (MDS) would be carried out using the software package GROMACS-2019 and the CHARMM36 force field (Adasme-Carreño, Muñoz-Gutierrez, Caballero, & Alzate-Morales, 2014; Pronk et al., 2013). The protein-ligand interaction was solvated, the system was neutralized, and the CHARMM-GUI program was used to produce the protein topology and parameter files of the ligand. The system undergoes 5000 steps of energy minimization using the gradient technique, followed by 125 ps of equilibrium at a preset number of molecules, volume, and temperature (NVT), Before the simulation was completed, the dynamic simulation would then be performed for 100 ns with a time-stage of 2 fs and a set number of molecules, pressure, and temperatures (310 K) for each simulation by using high-performance computing and calculating the Root Mean Square Deviation (RMSD), the number of hydrogen bonds and Radius of gyration (Rg) the of the protein-ligand complexes and proteins atom backbone.

III. RESULTS AND DISCUSSION

3.1 Molecular docking

The solved structures of the EGFR (PDB ID:1XKK) and VEGFR-2 (PDB ID:4ASD) were determined, and the process of molecular docking was carried out with auto dock vina software using 16 ligands extracted from the Drug Bank the server These ligands underwent geometry optimization, energy minimization, noncovalent interactions, Kollman charges with proteins and polar hydrogens atoms. The values with the highest docking scores and standard deviations were listed in Table 1 in which the results for EGFR indicated that SCHEMBL2747005, CHEMBL3739627, 1C, SCHEMBL2435793, and 2C had docking score values of -11.9, -11.98, -12.12, -12.2 and -12.42 (Kcal/mol) respectively, with standard deviation values of 0.06, 0.04, 0.07, 0.06 and 0.07. while the 3C compound had the highest docking score of value -12.48 (Kcal/mol) with a standard deviation value of 0.07.

On the other hand, the results for VEGFR-2 indicated that 4C, CHEMBL3739627, CHEMBL3740574, and 5C showed docking score values of -11.92, -12.02, -12.12, -12.44, and -12.46 (Kcal/mol) respectively, with standard deviation values of 1.04, 0.66, 0.83, 0.04 and 0.04. while the compound 3C had the best value of docking score of -12.52 (Kcal/mol) and a value of standard deviation of 0.26. So, the compound 3C was employed as a dual inhibitor for EGFR and VEGFR-2 kinases because, as shown in Table 1 it had a strong docking score and a better standard of deviation for both kinases.

Although, 3C had a structure of N-[4-fluoro-3-(trifluoromethyl) phenyl]-6-[2-(propanoylamino) pyrimidin-4-yl] oxynaphthalene-1-carboxamide and a formula of C25H18F4N4O3 which were arranged as shown in Figure 1.

EGFR			VEGFR-2		
Compound name	Compound CID	Docking score (Kcal/mol)	Compound name	Compound CID	Docking score (Kcal/mol)
sorafenib	216239	-10.04±0.04	sorafenib	216239	-11.01±0.02
Erlotinib	176870	-7.8±0.08	Erlotinib	176870	-7.93±0.08
Lapatinib	208908	-11.1±0.06	Lapatinib	208908	-10±0.54
Golvatinib (E7050)	16118392	-11.24±0.30	Golvatinib (E7050)	16118392	-8.74±0.18
Sunitinib	5329102	-8.96±0.04	Sunitinib	5329102	-8.21±0.46
Vandetanib	3081361	-9.02±0.09	Vandetanib	3081361	-8.5±0.29
SCHEMBL2747005	59813639	-11.9±0.06	4C	141505675	-11.92±1.04
CHEMBL3739627	127041171	-11.98±0.04	CHEMBL3739627	127041171	-12.02±0.66
1C	140166580	-12.12±0.07	CHEMBL3740574	127038479	-12.12±0.83
SCHEMBL2435793	67406704	-12.2±0.06	5C	161564964	-12.44±0.04
2C	86624925	-12.42±0.07	6C	90898392	-12.46±0.04
3C	159836869	-12.48±0.07	3C	159836869	-12.52±0.26

Table1: Docking scores (Kcal/mol) for EGFR and VEGFR-2 determined with Auto Dock Vina, the docking was performed 5 times for each ligand.

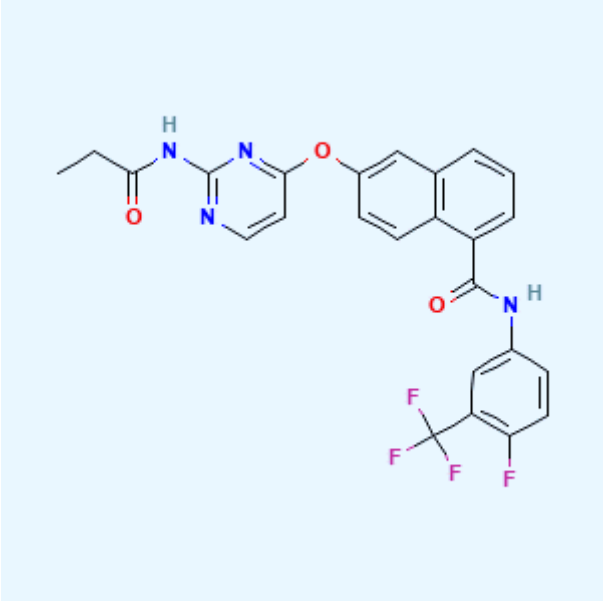

Figure 1: Chemical structure of 3C compound (produced from PUBCHEM server).

3.2 Drug Likeness Score:

By using the internet server Molsoft (http://molsoft.com/mprop/) the corresponding drug-likeness values for the compound 3C were calculated with value 0.97, MolLogP: 1.96, MolLogS: -2.98 (in Log(moles/L)) 116.15 (in mg/L), MolPSA: 7.99 A2, MolVol: 536.58 A3, pKa of most Basic/Acidic group: 0.91/ 11.64, BBB Score: 2.35 The Blood-Brain Barrier (BBB) Score: 6-High,0-Low and Number of stereo centers: 0, Figure 2

showed the drug-likeness curve in which the blue curve with maximum value equal 1 indicate that the compound was a drug, green curve indicate that the compound was non-drug and the red line indicated the drug-likeness score of 3C compound that equal 0.97 and near to 1 so 3C compound could be a drug.

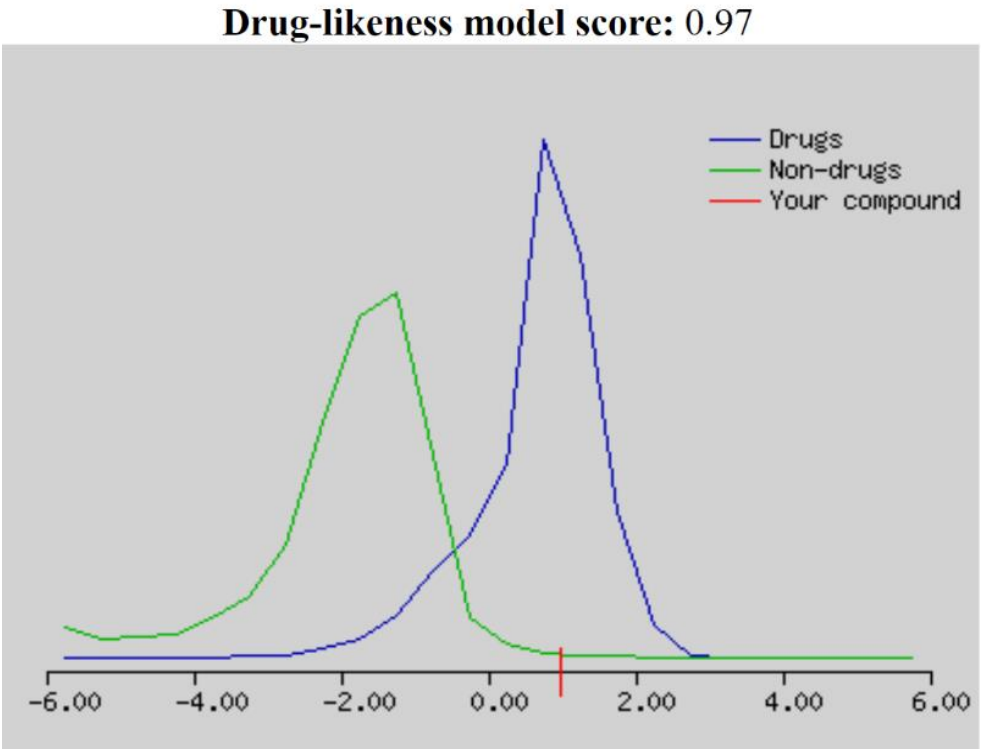

Figure 2. showed the drug likeness model score of 3C compound.

4.3 Pharmacokinetic (ADME) and toxicity

A highly active derivative with an in-silico report was used to evaluate the physicochemical characteristics of the suggested ADMET profile. Approaches using the pkCSM descriptor method were used to calculate it (Lipinski, Lombardo, Dominy, & Feeney, 2001). Good absorption qualities had been expected for molecules that followed not less than three of the next parameters from Lipinski's rule of five:

The partition coefficient (log P), the molecular weight, the number of hydrogen bond acceptors, and the number of hydrogen bond donors must not exceed five, 500, ten, and five, respectively (Aziz, George, El-Adl, & Mahmoud, 2022).

Based on the obtained data in Table 2 compound 3C had no violation in the list of prediction about the rule of five in which Molecular weight was 498.43 g/mol (> 500), the number of H-bond donors were 2, the number of H-bond acceptors are 9 and Log Po/w is equal 4.87 (> 5). There was no blood-brain barrier (BBB) in 3C, CYP1A2, CYP2C19, CYP2C9, CYP2D6, and CYP3A4 inhibitors were the vital enzyme involved in drug-metabolizing could be prevented by 3C, the Bioavailability Score were 0.55 and poor water Solubility, good results for 3C's water solubility show that oral administration is extremely unlikely (Delaney, 2004). These results were very important and great which made the 3C compound to be used as a cancer inhibitor.

The toxicity of a compound was determined by the toxicity test from the online server Preadmet shown in Table 3 in which Acute algae toxicity of 3C was very small with a value of 0.00467964, Ames test was non-mutagen, the Carcinogenicity (Mouse and Rat) was negative, low Acute daphnia toxicity of about 0.00448741 the in vitro hERG inhibition had a medium risk, Acute fish toxicity (minnow) was 5.83112e-005 and the Ames TA100_10RLI, TA100_NA, TA1535_10RLI, and TA1535_NA all were negative. Finally, we concluded that the results of 3C for Pharmacokinetic and toxicity were very good compared to the two references sorafenib and erlotinib of EGFR and VEGFR-2 respectively, so 3C had a high probability of being used as an inhibitor for the 2 kinases.

Physicochemical Properties		Water Solubility		Pharmacokinetics	
Formula	C25H18F4N4O3	Log S (ESOL)	-6.01	GI absorption	Low
Molecular weight	498.43 g/mol	Solubility	4.83e-04 mg/ml ; 9.68e-07 mol/l	BBB permeant	No
Num heavy atoms	36	Class	Poorly soluble	P-gp substrate	No
Num arom heavy atoms	22	Log S (Ali)	-6.82	CYP1A2 inhibitor	Yes
Fraction Csp3	0.12	Solubility	7.52e-05 mg/ml ; 1.51e-07 mol/l	CYP2C19 inhibitor	Yes
Num rotatable bonds	9	Class	Poorly soluble	CYP2C9 inhibitor	Yes
Num H-bond acceptors	9	Log S (SILICOS-IT)	-9.88	CYP2D6 inhibitor	Yes
Num H-bond donors	2	Solubility	6.50e-08 mg/ml ; 1.30e-10 mol/l	CYP3A4 inhibitor	Yes
Molar Refractivity	124.35	Class	Poorly soluble	Log Kp (skin permeation)	-5.71 cm/s
Consensus Log $P_{o/w}$	4.87	Bioavailability Score	0.55	Lipinski	Yes; 0 violation

Table 2. Pharmacokinetic (ADME) of high effective compound(2C) (generated by Swissadme server).

ID	Value
algae_at	0.00467964
Ames_test	non-mutagen
Carcino_Mouse	negative
Carcino_Rat	negative
daphnia_at	0.00448741
hERG_inhibition	medium risk
medaka_at	$5.86052e^{-005}$
minnow_at	$5.83112e^{-005}$
TA100_10RLI	negative
TA100_NA	negative
TA1535_10RLI	negative
TA1535_NA	negative

Table 3. Toxicity value of high effective compound(2C) (generated by PREADMET server).

3.4 Interaction Analysis between protein and ligand

With high-value docking scores of -12.48 Kcal/mol and -12.52 Kcal/mol, the 3C molecule binds to the active sites of EGFR and VEGFR-2, respectively. The 3D views from the docking procedure that appear in ribbon structures in Figure 3,4 illustrate interactions between the 3C and the known active sites of EGFR and VEGFR-2, respectively. The binding free energy was calculated by adding the covalent energies of four separate variables—the van der Waal, hydrogen bond, desolation, and electrostatic energies.

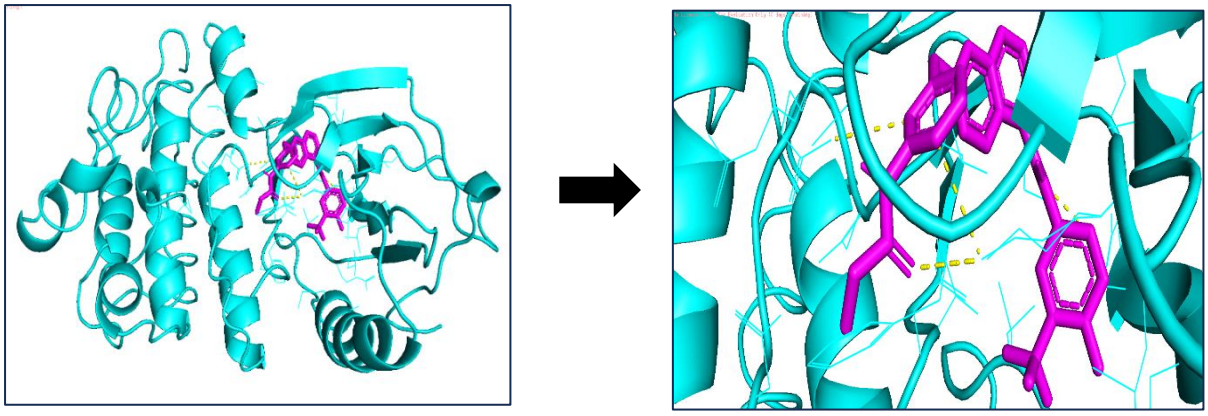

Figure 3: Binding of 3C at active site on EGFR kinase: Ribbon structures.

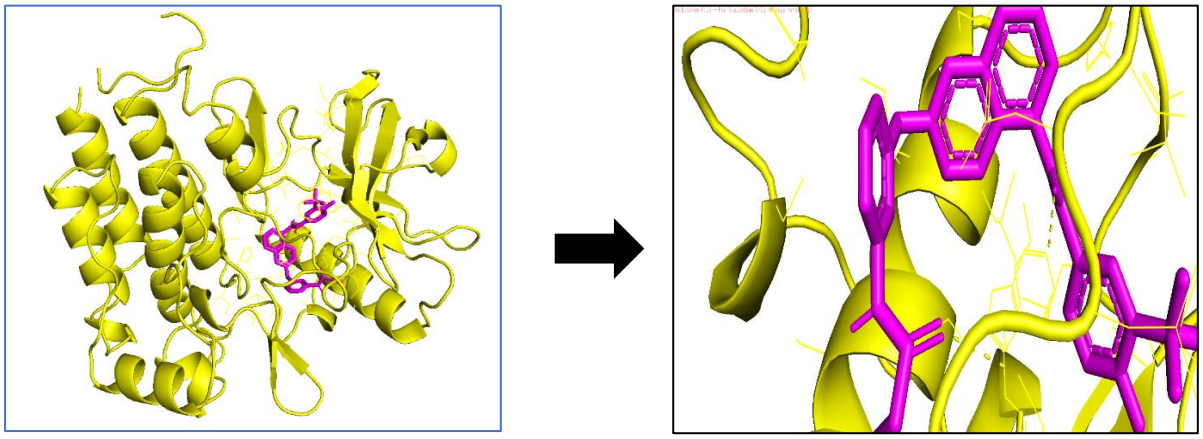

Figure 4: Binding of 3C at active site on VEGFR-2 kinase: Ribbon structures.

Using the PLIP server (Protein-Ligand Interaction Profiler), the interactions of 3C with EGFR and VEGFR-2 were examined. Hydrogen bonds, hydrophobic interaction, ionic bonds, and water bridges were the four types of bonding that make up the interface between a protein and its ligand. The importance of the hydrogen bond in ligand binding and drug selection. The major interactions between EGFR kinase active sites and 3C compound were shown in Table 4 in which there were (1) hydrophobic Interactions at LEU-718, PHE-723, VAL-726, ALA-743, LYS-745, LEU-788, THR-790, LEU-844 and LEU-858 residues with 3C compound. (2) Hydrogen Bonds: Drug selectivity, metabolization, and adsorption were all significantly influenced by hydrogen bonding that was performed at LYS-745 and THR-790 residues with 3C compound. (3) π-Cation Interactions were formed at LYS-745 residue with the aromatic group of the 3C compound. Figure 5 showed (a) the surface view and (b) the stereo view of the interaction between EGFR kinase and 3C compound that involved the 3 previous interactions.

(a) (b)

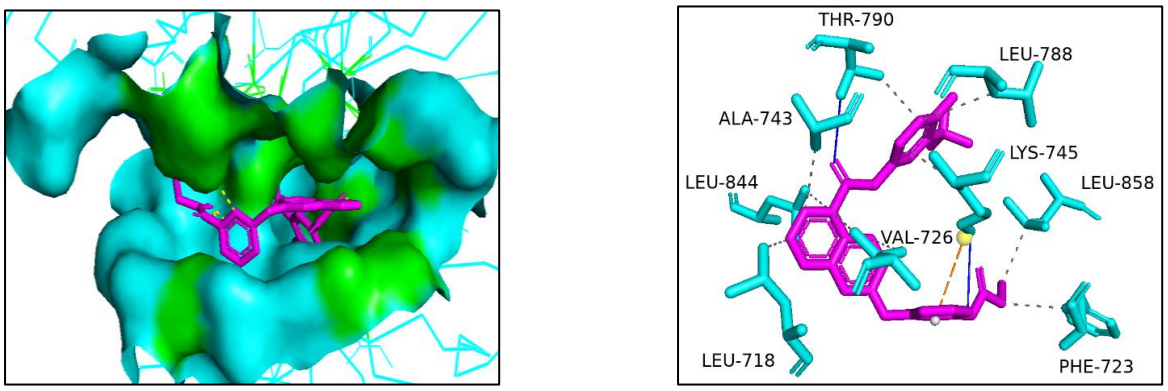

Figure 5: (a) The surface view of compound 3C (magenta) docked to the active site of EGFR (green). **(b)**Stereo view of H-bond, Hydrophobic Interactions, π-Cation Interactions and Halogen Bonds patterns of the EGFR amino acid that have active pocket residues (cyan)Binding 3C(magenta).

On the other hand, Table 5 showed a major interaction between VEGFR-2 kinase active sites and 3C compound these were (1) hydrophobic Interactions between 3C compound and 9 residues of amino acids these were LYS-868, ALA-881, GLU-885, ILE-888, LEU-889, VAL-916, ILE-1044, ASP-1046, and LEU-1049 residues. (2) Hydrogen Bonds that are responsible for drug specificity and ligand binding were illustrated between 3C compound and 5 residues of amino acids these were LYS-868, GLU-885, ASP-1046, ASP-1046, and LEU-1049 residues. (3) π-Cation Interactions that formed between the aromatic group of 3C compound and LYS-868 residue. Figure 6 shows the interaction between EGFR kinase and 3C compound that involved the 3 previous interactions (a) the surface view and (b) the stereo view. As a result, the 3C compound had better interactions with EGFR and VEGFR-2 kinases rather than sorafenib and erlotinib as references respectively, so had a great probability of being used as an inhibitor for the 2 kinases and treating cancer.

(a) (b)

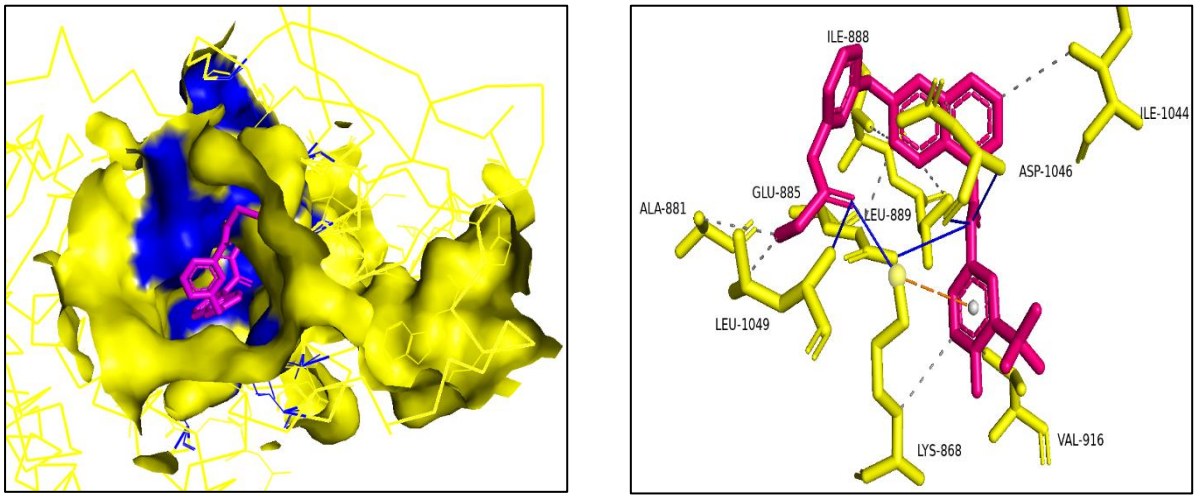

Figure 6: (a) The surface view of compound 3C (magenta) docked to the active site of EGFR (blue). **(b)**Stereo view of H-bond, Hydrophobic Interactions, π-Cation Interactions and Halogen Bonds patterns of the EGFR amino acid that have active pocket residues (yellow) Binding 3C (magenta).

3.2. Molecular dynamic simulation

A molecule's dynamic simulation offers information on possible changes in conformation over a trajectory that was equivalent to the biological environment. A computer simulation technique known as molecular dynamic (MD) simulation could be used to visualize the actual positions of atoms and molecules. We could therefore provide information on which molecular interactions on the generated compounds were stable

by using a molecular dynamics simulation. The simulation result was analyzed over structural analysis by RMSD, Rg, and the number of H-bonds. We utilized the GROMACS-2019 server and the CHARMM-GUI to obtain the protein topology and ligand parameter files to carry out molecular dynamic simulations. Before the simulation was finished, the system went through 5000 steps of energy minimization using the gradient technique, followed by 125 ps of equilibrium at a predetermined number of molecules, volume, and temperature (NVT). Finally, the dynamic simulation would be carried out for 100 ns with a time stage of 2 fs and a predetermined number of molecules, pressure, and temperatures (310 K) for each simulation. Molecular Dynamic Simulation was performed for 100 ns using the backbone VEGFR-2 and EGFR kinases, as well as EGFR-2C and VEGFR-2-2C complexes.

Figure 7 shows the root means square deviation (RMSD) and radius of gyration (Rg) graphs for EGFR kinase and EGFR-3C complex over the simulation time. If the system's components were sufficiently balanced during the simulation and if any deviations in the shape of protein from the initial structure could be detected, the RMSD value provided valuable information. In studies employing MD modeling, Rg had a key influence in determining how compact a protein was (Sargolzaei, 2021). According to Figure 7, the RMSD value of backbone EGFR kinase as a reference ranged between (0 and 0.3 nm) and EGFR-3C complex ranged between (0 and 0.22 nm) and became stable from (10 ns) to (100 ns) showed its stability along the simulation period, while Rg graph of backbone EGFR kinase as a reference had Rg value between (1.91 – 1.99 nm) and EGFR-3C complex had Rg value between (1.93 – 2.04 nm) with high compatibility and converging and low fluctuations for both showing a high stability of Rg analysis and high probability of using 3C compound as an inhibitor for cancer.

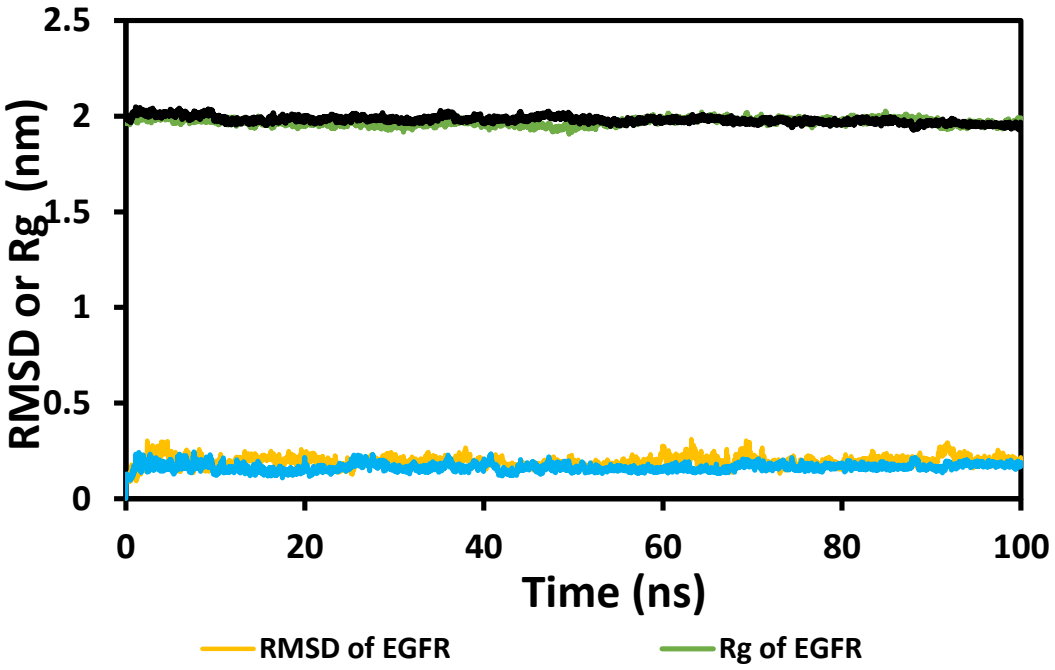

Figure7: Plot of root means square deviation (RMSD) and of radius of gyration (Rg) of backbone of EGFR and EGFR kinase-3C complex.

The radius of gyration (Rg) and root means square deviation (RMSD) graphs for the VEGFR-2 kinase and VEGFR-2 -3C complex were displayed in Figure 8 along with the simulation time, in which the RMSD value of the reference VEGFR-2 kinase's backbone ranged between (0 and 0.51 nm) and stabilized from (20 ns) to (100 ns), while the VEGFR-2 -3C complex ranged between (0 and 0.28 nm) and stabilized from (10 ns) to (100 ns), demonstrating its stability over each stage of the simulation. While the VEGFR-2 -3C complex had an Rg value between (1.99 - 2.04 nm) with great compatibility and converging and low variations, the Rg graph of backbone VEGFR-2 kinase as a reference had an Rg value between (1.99 – 2.14 nm), demonstrating a high stability of Rg analysis.

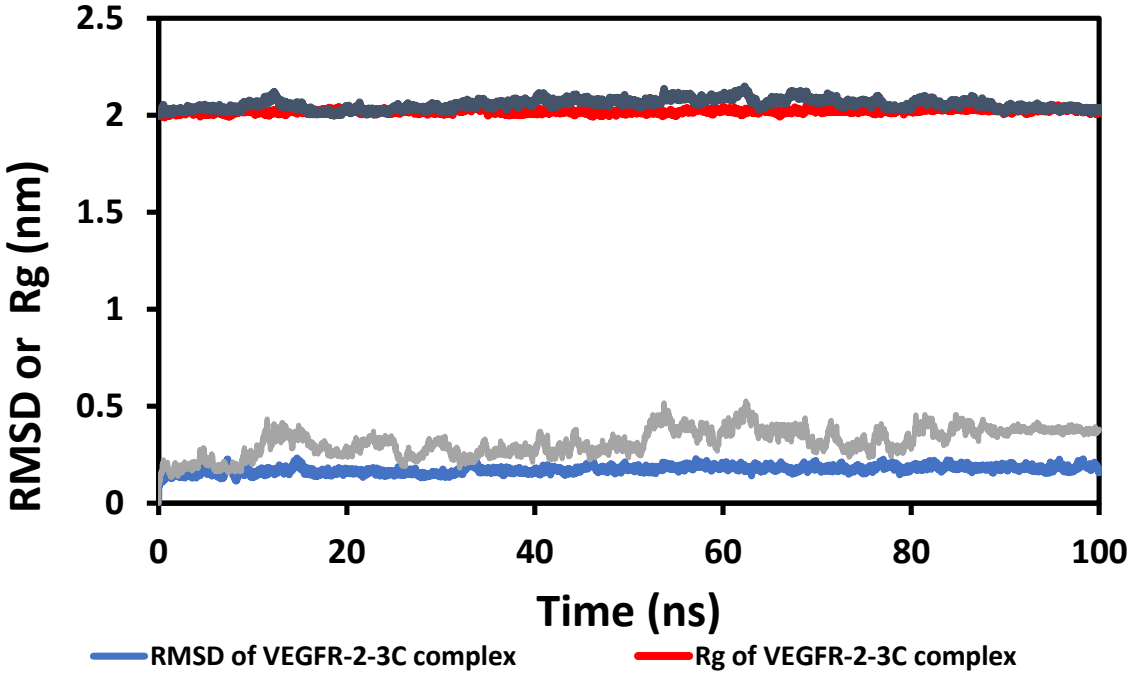

Figure 8: Plot of root means square deviation (RMSD) and of radius of gyration (Rg) of backbone of VEGFR-2 and VEGFR-2 kinase-3C complex.

In the final result, H-bond analysis utilizing MD simulation generated several hydrogen bond graphs. Since hydrogen bonds significantly affected metabolism, drug selectivity, adsorption, and other hydrogen-bonding properties, they had to be taken into account when designing drugs (Rajagopal & Vishveshwara, 2005). The varied pattern of the novel identified EGFR kinase-3C complex, with values ranging from 0 to 5 as shown in Figure 9. The observed variance in the number of H-bonds produced by the VEGFR-2 kinase-3C complex, which ranged from 1 to 4, was shown in Figure 10. When compared to the interactions between the ligand and the two proteins shown in the previous Tables (4, 5), which indicated approximately the same range of hydrogen bonds for the two complexes—roughly 2 for the EGFR and 5 for VEGFR-2—the results of this study were more favorable. As a result, the examination of the H-bonds for the 3C with the kinases had a good result, stabilizing the 2 complexes, increasing the chances that the 3C would be utilized as a dual inhibitor for EGFR and VEGFR-2 and eliminating cancer cells.

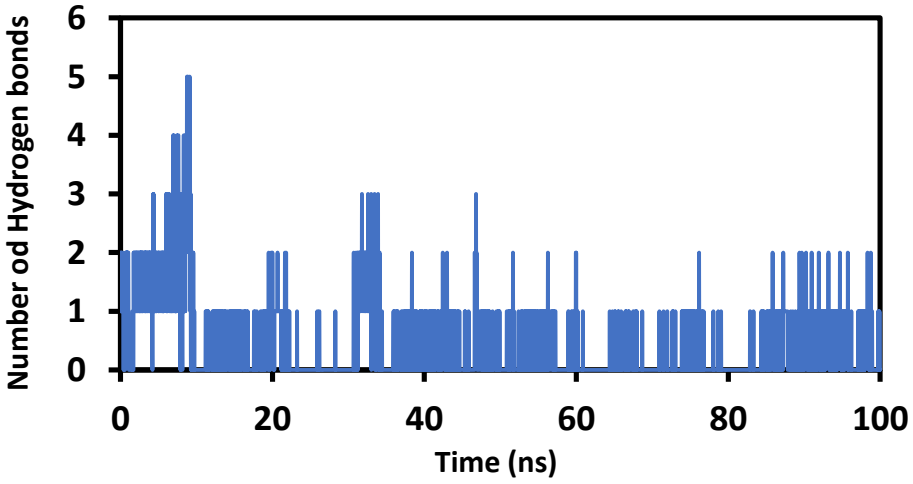

Figure 9: Number of H-bonds for EGFR kinase-3C complex formed during 100 ns MD simulation.

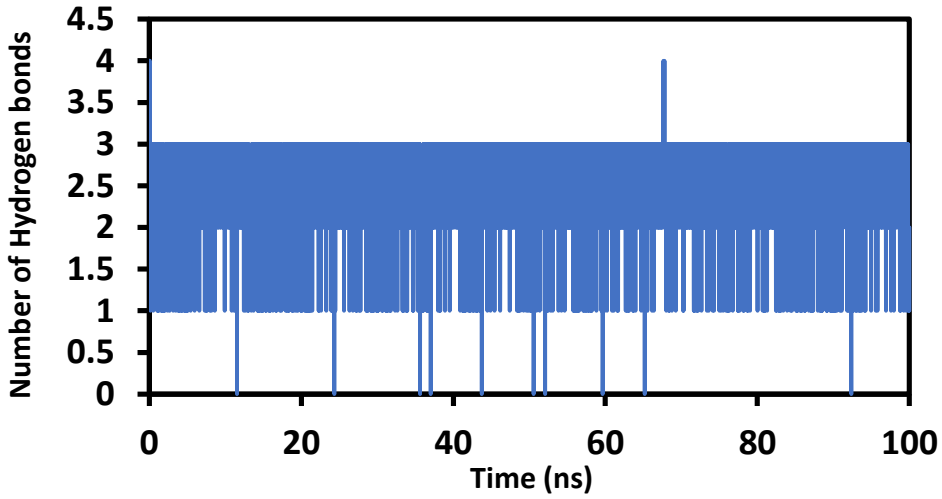

Figure 10: Number of H-bonds for VEGFR-2 kinase-3C complex formed during 100 ns MD simulation.

V –CONCLUION

The kinases of the EGFR and VEGFR-2 have been proposed as promising targets for cancer therapy. The goal of this technique was to find a substance that was more potent than the available drugs; as a result, all varieties of EGFR and VEGFR -2 inhibitors were obtained from a literature review. The effectiveness of compound 3C inhibits the EGFR and VEGFR-2 proteins is demonstrated by the molecular docking data with high values. Additional in vivo or in vitro study on the pharmacological and biological features of these ligands in cancer therapy that target EGFR and VEGFR-2 was required, which was why the drug similarity score, and pharmacokinetic analysis were demonstrated. The compound 3C with the two kinases produced the greatest results in the examination of ligand and protein interactions. A 3C compound's conformational changes throughout a time step were compared in the dynamic simulation. The great stability of the binding was confirmed by molecular dynamic simulation through the analysis of numerous parameters, including the RMSD, Rg, and number of H-bonds. These findings therefore confirmed the use of 3C in cancer chemoprevention as a dual inhibitor for EGFR and VEGFR-2 kinases.

REFERENCES

1. Adasme-Carreño, F., Muñoz-Gutierrez, C., Caballero, J., & Alzate-Morales, J. H. (2014). Performance of the MM/GBSA scoring using a binding site hydrogen bond network-based frame selection: the protein kinase case. *Physical Chemistry Chemical Physics, 16*(27), 14047-14058. doi:10.1039/C4CP01378F
2. Aziz, N. A. A. M., George, R. F., El-Adl, K., & Mahmoud, W. R. (2022). Design, synthesis, in silico docking, ADMET and anticancer evaluations of thiazolidine-2,4-diones bearing heterocyclic rings as dual VEGFR-2/EGFRT790M tyrosine kinase inhibitors. *RSC Advances, 12*(20), 12913-12931. doi:10.1039/D2RA01119K
3. Delaney, J. S. (2004). ESOL: Estimating Aqueous Solubility Directly from Molecular Structure. *Journal of Chemical Information and Computer Sciences, 44*(3), 1000-1005. doi:10.1021/ci034243x
4. Drake, J. M., Lee, J. K., & Witte, O. N. (2014). Clinical Targeting of Mutated and Wild-Type Protein Tyrosine Kinases in Cancer. *Molecular and Cellular Biology, 34*(10), 1722-1732. doi:10.1128/MCB.01592-13
5. Ferrara, N., Gerber, H.-P., & LeCouter, J. (2003). The biology of VEGF and its receptors. *Nature medicine, 9*(6), 669-676.
6. Hanwell, M. D., Curtis, D. E., Lonie, D. C., Vandermeersch, T., Zurek, E., & Hutchison, G. R. (2012). Avogadro: an advanced semantic chemical editor, visualization, and analysis platform. *Journal of Cheminformatics, 4*, 17 - 17.

7. Holmes, K., Roberts, O. L., Thomas, A. M., & Cross, M. J. (2007). Vascular endothelial growth factor receptor-2: Structure, function, intracellular signalling and therapeutic inhibition. *Cellular Signalling, 19*(10), 2003-2012. doi:https://doi.org/10.1016/j.cellsig.2007.05.013
8. Larsen, A. K., Ouaret, D., El Ouadrani, K., & Petitprez, A. (2011). Targeting EGFR and VEGF(R) pathway cross-talk in tumor survival and angiogenesis. *Pharmacology & Therapeutics, 131*(1), 80-90. doi:https://doi.org/10.1016/j.pharmthera.2011.03.012
9. Liang, X., Yang, Q., Wu, P., He, C., Yin, L., Xu, F., . . . Jing, B. (2021). The synthesis review of the approved tyrosine kinase inhibitors for anticancer therapy in 2015–2020. *Bioorganic Chemistry, 113*, 105011. doi:https://doi.org/10.1016/j.bioorg.2021.105011
10. Liao, B.-C., Lin, C.-C., & Yang, J. C.-H. (2015). Second and third-generation epidermal growth factor receptor tyrosine kinase inhibitors in advanced nonsmall cell lung cancer. *Current opinion in oncology, 27*(2), 94-101.
11. Linderholm, B. K., Hellborg, H., Johansson, U., Elmberger, G., Skoog, L., Lehtiö, J., & Lewensohn, R. (2009). Significantly higher levels of vascular endothelial growth factor (VEGF) and shorter survival times for patients with primary operable triple-negative breast cancer. *Ann Oncol, 20*(10), 1639-1646. doi:10.1093/annonc/mdp062
12. Lipinski, C. A., Lombardo, F., Dominy, B. W., & Feeney, P. J. (2001). Experimental and computational approaches to estimate solubility and permeability in drug discovery and development settings. *Adv Drug Deliv Rev, 46*(1-3), 3-26. doi:10.1016/s0169-409x(00)00129-0
13. Mohassab, A. M., Hassan, H. A., Abdelhamid, D., Gouda, A. M., Youssif, B. G. M., Tateishi, H., . . . Abdel-Aziz, M. (2021). Design and synthesis of novel quinoline/chalcone/1,2,4-triazole hybrids as potent antiproliferative agent targeting EGFR and BRAFV600E kinases. *Bioorganic Chemistry, 106*, 104510. doi:https://doi.org/10.1016/j.bioorg.2020.104510
14. Morris, G. M., Huey, R., Lindstrom, W., Sanner, M. F., Belew, R. K., Goodsell, D. S., & Olson, A. J. (2009). AutoDock4 and AutoDockTools4: Automated docking with selective receptor flexibility. *J Comput Chem, 30*(16), 2785-2791. doi:10.1002/jcc.21256
15. Musumeci, F., Radi, M., Brullo, C., & Schenone, S. (2012). Vascular Endothelial Growth Factor (VEGF) Receptors: Drugs and New Inhibitors. *J Med Chem, 55*(24), 10797-10822. doi:10.1021/jm301085w
16. N.C.I. (2023). (N.I.H.), Types of cancer treatment.
17. Organization, W. H. (2020). WHO report on cancer: setting priorities, investing wisely and providing care for all.
18. Otrock, Z. K., Makarem, J. A., & Shamseddine, A. I. (2007). Vascular endothelial growth factor family of ligands and receptors: Review. *Blood Cells, Molecules, and Diseases, 38*(3), 258-268. doi:https://doi.org/10.1016/j.bcmd.2006.12.003
19. Pronk, S., Páll, S., Schulz, R., Larsson, P., Bjelkmar, P., Apostolov, R., . . . Lindahl, E. (2013). GROMACS 4.5: a high-throughput and highly parallel open source molecular simulation toolkit. *Bioinformatics, 29*(7), 845-854. doi:10.1093/bioinformatics/btt055
20. Rajagopal, S., & Vishveshwara, S. (2005). Short hydrogen bonds in proteins. *Febs j, 272*(8), 1819-1832. doi:10.1111/j.1742-4658.2005.04604.x
21. Sarabipour, S., Ballmer-Hofer, K., & Hristova, K. (2016). VEGFR-2 conformational switch in response to ligand binding. *eLife, 5*, e13876. doi:10.7554/eLife.13876
22. Sargolzaei, M. (2021). Effect of nelfinavir stereoisomers on coronavirus main protease: Molecular docking, molecular dynamics simulation and MM/GBSA study. *Journal of Molecular Graphics and Modelling, 103*, 107803. doi:https://doi.org/10.1016/j.jmgm.2020.107803
23. Sarkar, S., Mazumdar, A., Dash, R., Sarkar, D., Fisher, P. B., & Mandal, M. (2010). ZD6474, a dual tyrosine kinase inhibitor of EGFR and VEGFR-2, inhibits MAPK/ERK and AKT/PI3-K and induces apoptosis in breast cancer cells. *Cancer Biol Ther, 9*(8), 592-603. doi:10.4161/cbt.9.8.11103
24. Schlam, I., & Swain, S. M. (2021). HER2-positive breast cancer and tyrosine kinase inhibitors: the time is now. *NPJ Breast Cancer, 7*(1), 56.
25. Schrodinger, L. (2021). he fPyMOLg molecular graphics system, version 2.5.
26. Sigismund, S., Avanzato, D., & Lanzetti, L. (2018). Emerging functions of the EGFR in cancer. *Molecular oncology, 12*(1), 3-20.
27. Sullivan, I., & Planchard, D. (2017). Next-generation EGFR tyrosine kinase inhibitors for treating EGFR-mutant lung cancer beyond first line. *Frontiers in medicine, 3*, 76.
28. Trott, O., & Olson, A. J. (2010). AutoDock Vina: Improving the speed and accuracy of docking with a new scoring function, efficient optimization, and multithreading. *Journal of Computational Chemistry, 31*(2), 455-461. doi:https://doi.org/10.1002/jcc.21334

29. Usui, T., Ban, H. S., Kawada, J., Hirokawa, T., & Nakamura, H. (2008). Discovery of indenopyrazoles as EGFR and VEGFR-2 tyrosine kinase inhibitors by in silico high-throughput screening. *Bioorganic & Medicinal Chemistry Letters, 18*(1), 285-288. doi:https://doi.org/10.1016/j.bmcl.2007.10.084
30. Wieduwilt, M. J., & Moasser, M. M. (2008). The epidermal growth factor receptor family: Biology driving targeted therapeutics. *Cellular and Molecular Life Sciences, 65*(10), 1566-1584. doi:10.1007/s00018-008-7440-8
31. Wishart, D. S., Feunang, Y. D., Guo, A. C., Lo, E. J., Marcu, A., Grant, J. R., . . . Wilson, M. (2017). DrugBank 5.0: a major update to the DrugBank database for 2018. *Nucleic Acids Research, 46*(D1), D1074-D1082. doi:10.1093/nar/gkx1037
32. Zhao, Y., Bilal, M., Raza, A., Khan, M. I., Mehmood, S., Hayat, U., . . . Iqbal, H. M. N. (2021). Tyrosine kinase inhibitors and their unique therapeutic potentialities to combat cancer. *International Journal of Biological Macromolecules, 168*, 22-37. doi:https://doi.org/10.1016/j.ijbiomac.2020.12.009